

# Efficient dehazing method for large scale remote sensing images

## - Final Project Report -

Anouar Oussalah  
CentraleSupélec

[anouar.oussalah@student-cs.fr](mailto:anouar.oussalah@student-cs.fr)

Louis Chirol  
CentraleSupélec

[louis.chirol@student-cs.fr](mailto:louis.chirol@student-cs.fr)

### Abstract

*Haze is a common problem in satellite images that can obscure important details and make them difficult to interpret. It is caused by the scattering of light by particles in the atmosphere such as dust, smoke, and water vapor. Image dehazing is the process of removing the visual effects of atmospheric haze from images. In this paper, we present a method for image dehazing using the dark channel prior. The dark channel prior is a statistical property of natural images that states that in most natural images, there exists a small fraction of pixels with low intensity values in at least one color channel. This property has been successfully used in a variety of image processing tasks, including dehazing, denoising, and enhancement. Our method consists of four steps: preprocessing, atmospheric light estimation, dark channel calculation, and transmission map estimation. We apply our method to a variety of images and show that it is able to effectively remove the haze and improve the visibility and clarity of the images. Our method is fast and easy to implement, and has the potential to be used in a variety of applications such as satellite image analysis, object detection, and environmental studies.*

## 1. Introduction and motivation

The few last years have seen the availability of satellite images to explode, thanks to public initiatives such as the Copernicus program and the associated Sentinel satellites launched by the European Spatial Agency. This tremendous amount of data, consisting in high resolution images with relatively small revisit time, require new processing techniques to be valued, as they have the potential to provide a nearly real time monitoring of many human activities at the global scale.

On the other hand, due to major crisis such as climate change, risks over these activities are today unprecedented, as for instance floodings, wildfires or droughts are expected to become more and more frequent and intense in the close future. In this context, remote sensing may become a precious ally in monitoring almost day to day the evolution of such situations.

However, this nearly real time monitoring can be wasted by a poor quality of the images captured. In the case of hyperspectral satellites such as Sentinel-2, whose bands of acquisition range from 494.4 nm to 1373.5 nm, the images can be severely obstructed by clouds or haze, for several passes in a row, having as a consequence a dramatic collapse in the time frequency of exploitable images (see Figure 1). In this scope, Visual Computing techniques have a big potential to help dealing with such issues, as they provide interesting methods to process or improve images, without the drawbacks that Deep Learning can have, e.g being time greedy, computationally intensive, and not always robust to new data.

## 2. Problem definition

Haze is a common problem in satellite images that can obscure important details and make interpretation difficult. Haze is caused by the scattering of light by particles in the atmosphere, such as dust, smoke, and water vapor. This scattering causes the images to appear hazy or blurry, and can also cause a loss of contrast and color distortion.

The removal of haze from satellite images is an important task that can improve the visibility and clarity of the images. There are several methods for removing haze from images, including physical models, image enhancement techniques, and image restoration methods. In this paper, we present a fast algorithm for removing

haze from satellite images using the dark channel prior.

The dark channel prior is a statistical property of natural images that states that in most natural images, there exists a small fraction of pixels with low intensity values in at least one color channel. This property has been successfully used in a variety of image processing tasks, including dehazing, denoising, and enhancement.

The problem tackled in this paper will then be the following: evaluate the quality and time efficiency of recent Visual Computing methods from the literature ([2],[1], [8]), in order to find a satisfactory tool for haze removal in remote sensing images, in order to preserve the time frequency of exploitable images. More specifically, we will use [4] as a starting point and will refer to their paper and method all across this work, as our main source article.

### 3. Related work

In the field of image dehazing, there have been many methods proposed for removing haze from images. Some of the most popular methods include physical models, image enhancement techniques, and image restoration methods. Physical models such as the single scattering model and the multi-scale scattering model aim to estimate the physical properties of the atmosphere and the scattering of light by the atmosphere, and use these estimates to remove the haze from the images. Image enhancement techniques such as contrast enhancement and color correction aim to improve the visual quality of the images by adjusting the intensity and color values of the pixels [3]. Image restoration methods such as the dark channel prior [4], [2] and the fast atmospheric scattering transmission (FAST) [5] model aim to estimate the transmission map and recover the scene radiance from the hazy images. These methods have been shown to be effective in removing haze from images, but may be computationally expensive and may not always produce satisfactory results.

In this project, we mainly focus on the method developed by [4].

## 4. Methodology

### 4.1. Background

#### 4.1.1 The haze image model

Haze is traditionally an atmospheric phenomenon in which dust, smoke, and other dry particulates suspended in air, make light scatter. Thus, the observed image by satellite contains both the haze information and the ground features. In computer vision, the commonly used model to describe haze image [6] is the



Figure 1. Clean (upper) vs hazy (lower) Sentinel-2 images of agricultural fields close to Paris Saclay

following, for a given pixel  $x$  :

$$\mathbf{I}(x) = \mathbf{J}(x)t(x) + \mathbf{A}(1 - t(x)) \quad (1)$$

where  $\mathbf{I}$  stands for the observed intensity,  $\mathbf{J}$  is the scene radiance,  $\mathbf{A}$  stands for the atmospheric light of the whole image,  $t$  is the medium transmission coefficient, representing the portion of the light that is not scattered and reaches the imaging instrument. Therefore, in order to remove haze and recover the original image, we need to get the  $\mathbf{J}$  component. However, this is an ill-posed problem, because we don't really know  $\mathbf{A}$  and  $t$ .

#### 4.1.2 Dark Channel Prior

The dark channel prior is based on the following observation on outdoor haze-free images: In most of the non-sky patches, pixels in at least one color channel (r, g or b) have a low intensity value and close to zero. The low intensity in the dark channel is mainly due to the fact that natural images are colorful and full of shadows. For a given image  $J$ , we can then define its dark channel  $J^{dark}$  as follows:

$$J^{dark} = \min_{y \in \Omega(x)} (\min_{c \in \{r,g,b\}} J^c(y)) \quad (2)$$

where  $J^c$  is a color channel of the image  $J$ , and  $\Omega(x)$  is a local path centered at  $x$ . This observation was done on outdoor images in [2]. We will confirm this dark channel prior for satellite images, in the following section.

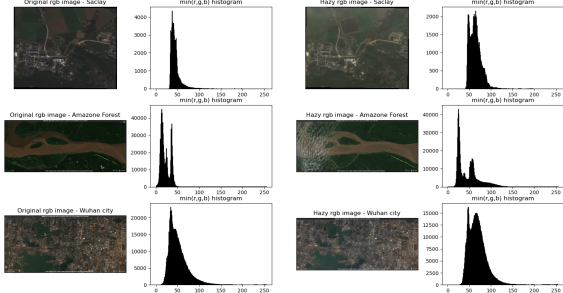


Figure 2. RGB image and histograms of the per-pixel minimum channel value for similar haze-free and hazy scenes. Top: Saclay plateau; middle: the Amazone; bottom: Wuhan, China

#### 4.1.3 Dark Channel prior verification on satellite images

The Dark Channel Prior technique for haze removal has been previously shown to be effective on natural images. However, its applicability to satellite images remains uncertain. In this study, we investigate the validity of the Dark Channel Prior assumption on satellite images of diverse landscapes (Saclay agricultural fields, Amazon forest, and Wuhan City). Citing [2], the dark channel hypothesis is : "in the statistical observation of the haze-free outdoor images that in most of the pixels of the non-sky patches, at least one color channel has very low intensity at some pixels". For this purpose, we will plot the histograms of the minimum value of each channel (r,g,b) of the pixels of some satellite images in various landscapes: the Saclay plateau, the Amazone forest and river, and the city of Wuhan, China, each time for an image with little haze and a hazy image of the scene, as in 2.

In the three haze free images, a significant part of the pixels have their minimum channel value below 50, whereas in the hazy version of the scene, this minimum value is in majority above 50, except for the Amazone image (yet, it's not so hazy, which can explain it). Thus, we will consider that our satellite images do verify the dark channel hypothesis, and that we can apply the dehazing method.

#### 4.1.4 Steps to recover the dehazed image

##### A) Estimate the Atmospheric Light

The atmospheric light is best estimated in the most haze-opaque region [7]. We choose the brightest 0.1% pixels in the dark channel, and select the one with highest intensity in the input image as the global atmospheric light. We compute the dark channel of the input haze image and estimate the global atmospheric

light using the pixel with the highest dark channel value:

$$\mathbf{A} = I(\mathbf{x}_k), \quad (3)$$

where  $\mathbf{x}_k = \arg_{\mathbf{x}} \max(I^{\text{dark}}(\mathbf{x}))$ .

##### B) Estimate the Coarse Atmospheric Veil

The atmospheric veil  $V(\mathbf{x})$  is defined as  $1 - t(\mathbf{x})$  and represents the additive airlight in a scene image. The haze imaging model is rewritten as

$$\mathbf{I}(\mathbf{x}) = \mathbf{J}(\mathbf{x})t(\mathbf{x}) + \mathbf{A}V(\mathbf{x}) \quad (4)$$

and normalized by dividing the global atmospheric light in each color channel separately to get

$$\frac{I^c(\mathbf{x})}{A^c} = \frac{J^c(\mathbf{x})}{A^c}t(\mathbf{x}) + V(\mathbf{x}) \quad (5)$$

The normalized image is restricted to  $[0, 1]$  with linear stretch method.

The atmospheric veil is subjected to two constraints: it is positive, and it cannot be higher than the minimum color component of  $\frac{I(\mathbf{x})}{A}$ . Using the dark channel prior ( $J^{\text{dark}}(\mathbf{x}) \approx 0$ ), the atmospheric veil and transmission are extracted by taking the minimum operation on equation (5), to both three color channels and the local patch (we assume that the atmospheric veil and transmission in a local patch  $\Omega(\mathbf{x})$  is constant, and we denote it  $\tilde{V}(\mathbf{x})$ ). Therefore, the atmospheric veil is extracted as

$$\tilde{V}(\mathbf{x}) = \min_{\mathbf{y} \in \Omega(\mathbf{x})} \left( \min_{c \in \{r,g,b\}} \frac{I^c(\mathbf{y})}{A^c} \right) \quad (6)$$

We will only take the minimum on the three color channels, as it was done in [?], which gives:

$$\tilde{V}(\mathbf{x}) = \min_{c \in \{r,g,b\}} \frac{I^c(\mathbf{x})}{A^c} \quad (7)$$

##### B) Refine the Atmospheric Veil using Gaussian Filter

To estimate the atmospheric veil  $V(\mathbf{x})$  from image  $\frac{I^c(\mathbf{x})}{A^c}$ , we use a low-pass Gaussian filter to smooth the result and prevent halo artifacts. The refined veil is represented by

$$V(\mathbf{x}) = \frac{1}{W^g} \sum_{\mathbf{y} \in S} G_\sigma(|\mathbf{x} - \mathbf{y}|) \tilde{V}(\mathbf{y}), \quad (8)$$

where  $G$  is a Gaussian function and  $\sigma$  is the size of the neighborhood used to smooth a pixel. The transmission is then easily calculated as

$$t(\mathbf{x}) = 1 - V(\mathbf{x}) \quad (9)$$

### B) Recover the Haze-free Image

We use global atmospheric light and transmission to recover the scene radiance, but noise can occur due to the proximity of the coarse atmospheric veil to zero. To address this, we use a lower bound  $t_0$  to restrict the transmission  $\mathbf{x}$  and  $k$  to keep a small amount of haze for distant objects. We also use a piecewise nonlinear stretch method to increase contrast in the final image. Therefore, we get:

$$\mathbf{J}(\mathbf{x}) = \mathbf{A} \times \frac{\mathbf{I}(\mathbf{x})/\mathbf{A} - kV(\mathbf{x})}{\max(t(\mathbf{x}), t_0)} \quad (10)$$

The full process is outlined in Algorithm 1 of Appendix A. The steps of the algorithm are illustrated in Figure 3

## 4.2. Data collection

It might be hard to find both a place and a date with haze to download a satellite image. We worked on the free SentinelHub EO Browser platform (<https://apps.sentinel-hub.com/eo-browser/>), which provides a free navigator for different satellite products (Sentinel, Landsat, MODIS...) and enables to visualize them at different dates. It made quite easy to target an area of interest (for instance, the Amazone), and to search back in time for hazy images and close haze-free shots of the same place. When we only needed the RGB part of the image, we used the built-in downloading tool, but when we needed the whole bands of a given raster, we ran a custom script calling the Google Earth engine API in a Google Colab Jupyter notebook, in order to export the raster for the desired dates, clipped on the area of interest drawn as a shapefile in the free, open source software QGIS (<https://www.qgis.org/fr/site/>).

Consequently, we were able to download a great variety of satellite hazy images and their haze free counterpart, both in RGB format or multispectral format. We also took screenshots of the satellite views used in our source article [4], to run our code in it and compare the output to the authors' results (see below).

## 5. Evaluation and extension of the method

In the last few years, it has become easy to export publicly available satellite images for given places and time periods. Thus, we will constitute a dataset of hazy Sentinel-2 hyperspectral images. The advantage of this source of data is that it is free and it covers a large part of the world's surface, so it can be used to generate very

diverse datasets, for instance urban, forest, fields or mountain images. This will enable us to constitute a diversified set of images, to evaluate the chosen method's capacity to adapt to any context. Moreover, we will try to evaluate if the reconstructed image is physically relevant, that is to say the histograms of values for each band of wavelength in similar to the same image in a haze free situation at a close acquisition date. Indeed, a lot of post-processing is often necessary on satellite images, for instance to derive vegetation or moisture index from multiple bands, so we will have to control how the methods influence the values. Finally, we will try to apply the method to other spectral bands than the classical RGB bands, specifically infrared bands available in the Sentinel-2 product, that enables us to compute the above mentioned physical indexes. We also try to extend the method to more than 3 bands at once, to dehaze a multispectral satellite cube.

The experiments that will be carried out are :

- Evaluate the influence of the diverse parameters involved in the method
- Evaluate the quality of the reconstruction, in terms of histograms over all the bands available
- Evaluate the relevance of a contrast enhancement step, as mentioned in our source article [4]
- Evaluate the time efficiency of the methods, to see which is most suitable for large scale processing
- Apply the method to other spectral bands of the Sentinel-2 product
- Extend the method to more than 3 channels at once

## 5.1. Parameters study

One question that our reference article did not tackle is how do the different parameters involved in the radiance restoration influence the final result. Thus, we separately examined the impact of  $k, \sigma, t_0$ .

We first tuned  $k$  on one image : this value, as it appears in the expression of  $J$  the restored radiance, lowers the resulting image pixel values, or equivalently shifts the histograms to the left. It is logical as a hazy image has a white veil one wants to remove, thus its pixel values are too high at haze points. Our experiments show indeed this effect with fixed  $\sigma$  and  $t_0$  values, up to the point where the image gets very dark. We found that values of  $k$  between 0.6 and 2 are often giving good results.

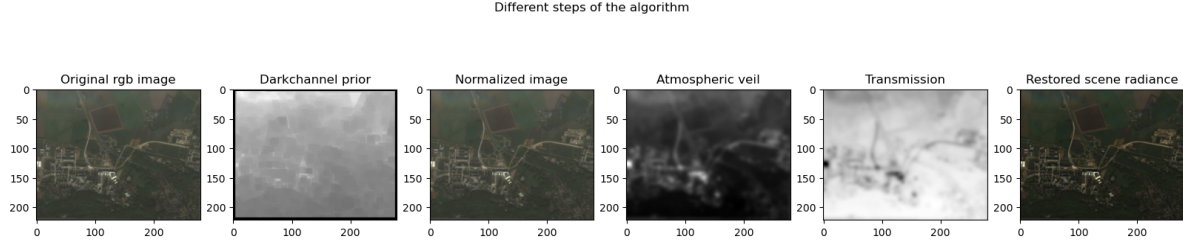


Figure 3. The different steps of the algorithm, from the hazy image to the restored radiance, on a view of the Saclay plateau zone

We then tried to modify the  $\sigma$  parameter, with an arbitrary value (not tuned) for  $k$ . It seemed that tuning the  $\sigma$  parameter helps to brighten the output image. We then verified it on our reconstruction with a better  $k$  parameter. We noticed that a too low value for  $\sigma$  results in a dark output image. However, with  $\sigma \geq 2$ , there are almost no noticeable effects of the parameter on the restored radiance or the histograms. We decided to set a reasonably high value ( $\sigma = 3$  for instance) for the rest of the study.

We finally inspected the influence of  $t_0$ , first with a small  $k$  value. The  $t_0$  parameter seems to brighten the restored radiance, as it shifts the histograms to the right, up to the point that we go back to the initial image with  $t_0$  close to 1. It is quite obvious using the formulas of the model, as  $J(x) = A * \frac{I(x)/A - k*V(x)}{\max(t(x), t_0)}$ , with  $t_0 \simeq 1$ , one gets  $J(x) \simeq I(x) - k*V(x)$ , which is  $J(x) \simeq I(x)$  with the little  $k$  value used here. Thus, we did the same with our tuned  $k$  parameter to better understand the potential interest of this parameter : we noticed the same brightening effect. The restored radiance with a little  $t_0$  is a bit too dark compared to a similar image (hazeless) of the same place, but too high value seem too bright and a bit hazy as well. An in-between value of  $t_0 = 0.6$  yields visually satisfying results, and histograms more similar to the haze-free shot of the place, yet a bit wider and with a slightly different mean.

As these experiments would take a large place in this report if we included all the images, we only provide the final result after tuning in Figure 4, and we invite the reader to play with the notebook (just running it to reproduce our experiments) to better see the influence of the parameters visually speaking.

## 5.2. Quality of the reconstruction

A first step to validate our implementation of the algorithm was applying it to the original paper's images. We did so in Figure 5. We saw that our result were quite relevant visually, yet quite different from

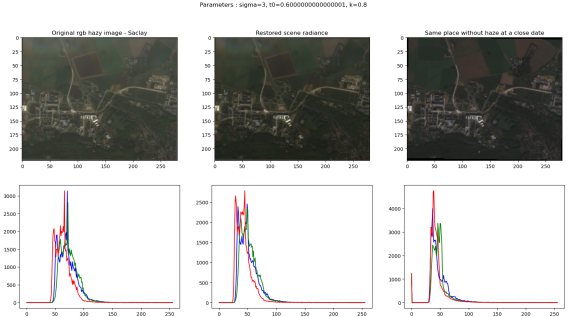


Figure 4. The dehazing of the RGB spectral bands after tuning the parameters. Top: the original, dehazed images and a close-date haze-free shot of the same place; bottom: the corresponding histograms.

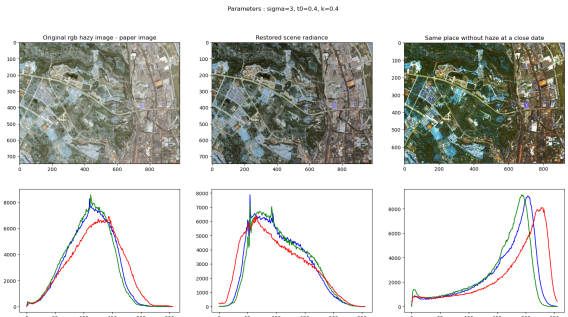


Figure 5. Top: a hazy image from the source paper, our dehazed image, and the author's dehazed image. Bottom: the corresponding histograms

the authors' one. Our guess for this difference was the mention of a contrast enhancement step in the paper after the dehazing, which we investigate in the following subsection. However, we decided to keep our implementation as the results seemed quite correct.

## 5.3. Contrast enhancement

For this part, we tested two different ways to improve contrast, using `cv2` library. The results obtained from the application of the two contrast enhancement functions on the recovered image showed that neither of them was able to produce an output that closely re-

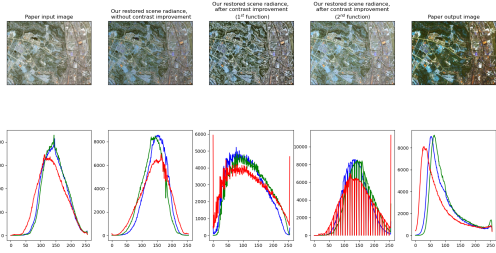


Figure 6. Top: a hazy image from the source paper, our dehazed images with enhanced contrast, and the author’s dehazed image. Bottom: the corresponding histograms

sembles the one presented in the reference article (see Figure 6) . Nevertheless, our output image using the first contrast enhancement function provided a visually pleasing dehazing result, appearing more natural than the image from the article. Despite its appealing appearance, we decided to use the restored radiance without contrast enhancement, as the histograms seemed to be excessively distorted, which could lead to the alteration of crucial physical information contained within the satellite image.

#### 5.4. Time efficiency

The algorithm was implemented on a MacBook Air M2 and tested on a variety of hazy images. The results indicate that the entire process of dehazing, including all necessary steps, took less than 1 second to complete on average. This highlights the potential for real-time applications of this technique, as well as its suitability for processing large image datasets. With much bigger images than the ones we used (typically 300x300, 600x1280 pixels images).

However, it is important to note that fine-tuning of hyperparameters for each image is required, which can be time-consuming.

#### 5.5. Comparison with other dehazing methods

In one of our latest experiment, we Github Copilot to write us a dehazing method and compared its results to the ones from our paper of reference. Unfortunately, the results were quite disappointing as the recovered image lacked the original colors and the histogram was unrecognizable (Figure 7). It seems like we still need human-written algorithms for dehazing purposes, at least for now.

Except for this method, we did not find convincing implementations of other dehazing methods, and it seems the dark channel prior is a widely used algorithm for this task. One way to quickly remove the

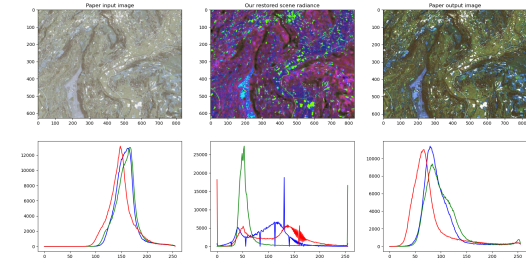


Figure 7. Top: a hazy image from the source paper, Github Copilot dehazed image, and the author’s dehazed image. Bottom: the corresponding histograms

white aspect of an image would be to normalize it, doing  $\frac{x - \min(x)}{\max(x) - \min(x)}$ , but it would distort the histograms too much. We missed some time to find other methods for comparison purposes.

#### 5.6. Application to other spectral bands

For the moment, we only applied our dehazing method to the RGB bands of our satellite images, as in most applications of dehazing in the litterature. But the Sentinel-2 product offers more spectral bands, in the infrared spectrum. These bands are of high interest for Earth observation and land monitoring purposes. For instance, the NIR band and the Red band can be combined to get a Normalized Difference Vegetation Index ( $NDVI = \frac{NIR - Red}{NIR + Red}$ ), which is widely used in remote sensing to monitor the vegetation. As land monitoring often requires timeseries, and as cloud obstruction and haze may represent outlier values in these time series, dehazing other spectral bands of the satellite images could prove to be useful to maintain as many correct points as possible in them, preventing these outliers.

Consequently, we tried to replace the Blue band in our input image by the NIR band of the Sentinel-2 product, then computing the NDVI from the restored image and comparing it to the NDVI of a hazeless image. The results are satisfying once again both visually and in terms of histograms. The mean of the histogram of the restored NDVI is shifted to the level of the haze free comparison image, and the modes of the two histograms are similar, as one can see in Figure 8. We can assert that the dark channel dehazing method does not distort the physical properties of the image.

Finally, we inspected how the method behaves on the other spectral bands. We used three of the 20m resolution bands, B6 (vegetation red edge, 740.4nm cen-

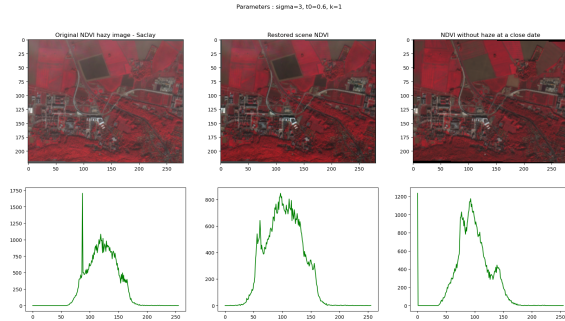


Figure 8. Dehazing of the NIR, Red and Green bands (top), and corresponding histograms of the NDVI computed from the NIR and Red bands (bottom)

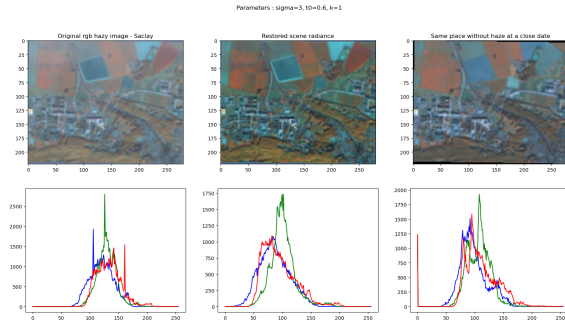


Figure 9. Dehazing of the Vegetation red edge (plotted in red), Narrow SWIR (plotted in green) and SWIR bands (plotted in blue) (top), and corresponding histograms (bottom)

tral wavelength), B11 (narrow SWIR, 1613.7nm central wavelength) and B12 (SWIR, 2202.4nm central wavelength). Once again, the method is appealing. The restored radiance is visually satisfying, and the histograms are shifted towards a shape closer to the haze-free shot of the scene (especially the red edge and second SWIR histograms whose skewness is increased to the left). The results are shown in Figure 9.

As a whole, those experiments confirm the potential for the dark channel prior dehazing method to efficiently remove haze over all the spectral bands of a satellite image, conserving its physical properties based on the bands histograms, when compared to a haze free image.

### 5.7. Extension to more than 3 channels

The last experiment we carried on satellite images was trying to dehaze the whole set of spectral bands at once, instead of applying the method to a set of three bands as in the original method. Indeed, when looking at the algorithm, only the dark channel prior and the atmospheric veil computation are dependent

on the RGB channels. However, it appeared that our code required no adaptation to work with multispectral images, as the numpy operations used on the RGB channel (min and max) are suited for more dimensions. Thus, we only introduced another pipeline function and a plot function dedicated to multispectral images. We then run those functions of 10-bands satellite images of the Saclay plateau.

We find that the method is working nicely on the multispectral image. The dark channel, the veil and the transmission are a bit blurry, but with a tuned value of  $k$ , all the 10 bands histograms are simultaneously aligned with the ones of haze free image (see Figure 10). It is harder to judge visually the dehazing on a gray scale for each band, but on the second plot (the steps detail), where we kept only the RGB channels for the original image, the normalized image and the restored radiance, it seems that the dehazing works as well as previously in this work.

As a conclusion, this dark channel prior based dehazing algorithm works well on multispectral images, without any need to sub-segment it into 3 bands images.

## 6. About the code provided

We provide a GitHub repository for this project. In this repository, you will find the jpg and raster images used throughout this work, the utility functions we built for implementing the method and plotting the results, and a Jupyter notebook (provided without plots for GitHub memory considerations), that you can play with to reproduce our results or to try to parametrize and apply the method on our images (link to the Github repo).

## 7. Conclusion

In this project, we presented a fast algorithm for removing haze from satellite images using the dark channel prior. The algorithm consists of the following steps: preprocessing, atmospheric light estimation, dark channel calculation, transmission map estimation, and recovery of the haze-free image. We have tested the algorithm on a variety of satellite images and obtained good results in terms of haze removal and image quality. The algorithm is able to effectively remove the haze from the images and improve the visibility and clarity of the images.

Our main contribution is that, step after step, we found that the method is not only suited for dehazing other spectral bands than the RGB channels of our

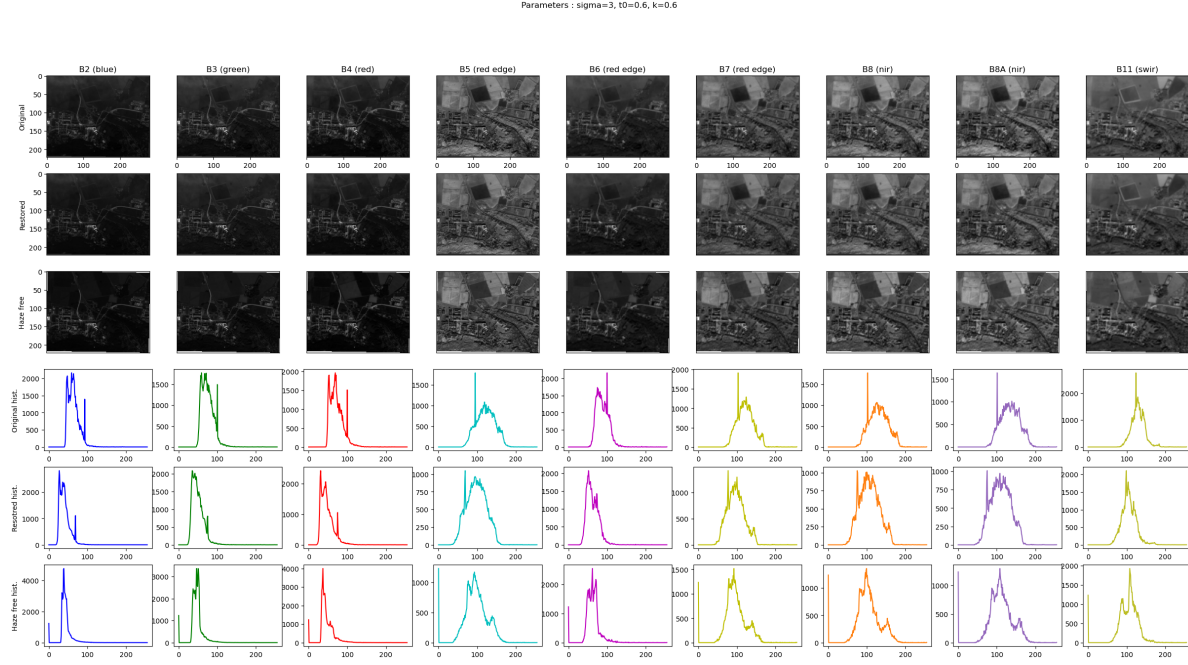


Figure 10. Dehazing results of a 10-bands multispectral image

images, but that it can be extended to dehaze all the bands of a multispectral image (like a Sentinel-2 acquisition) at once, without any adaptation, and yielding physically coherent results in terms of histograms for each spectral band. Consequently, this method could potentially be used in a preprocessing pipeline of satellite images time series, in order to restore the quality of hazy images of the series, in order to avoid outliers due to haze, for instance in crop monitoring where cloud obstruction already damages the time resolution of the series.

A nice addition to this work could have been to verify such a potential over the NDVI time series of a given crop plot across a year, and to confirm that the dehazing would preserve the smoothness of the curve. Another possibility of further work could be an automatic tuning or a decision rule for the value of the  $k$  parameter which is the most influent in the dehazing.

## References

- [1] Hyeongseok Choi, Heunseung Lim, Soohwan Yu, and Joonki Paik. Haze removal of multispectral remote sensing imagery using atmospheric scattering model-based haze thickness map. pages 1–2, 2020.
- [2] Kaiming He, Jian Sun, and Xiaou Tang. Single image haze removal using dark channel prior. *IEEE Transactions on Pattern Analysis and Machine Intelligence*, 33(12):2341–2353, 2011.
- [3] Eko Prasetyo Kartika Firdausy, Tole Sutikno. Image enhancement using contrast stretching and on rgb and ihs digital image. 2007.
- [4] Jiao Long, Zhenwei Shi, and Wei Tang. Fast haze removal for a single remote sensing image using dark channel prior. pages 132–135, 2012.
- [5] Dengyin Zhang Mingye Ju, Zhenfei Gu. Single image haze removal based on the improved atmospheric scattering model. *Neurocomputing*, 260:180–191, 2017.
- [6] S.G. Narasimhan and S.K. Nayar. Vision and the atmosphere. *Int'l J.Computer Vision*, 48:233–254, 2002.
- [7] S.K. Nayar S.G. Narasimhan. Contrast restoration of weather de graded images. *IEEE Trans. Pattern Analysis and Machine Intelligence*, 25:713–724, 2003.
- [8] Chi Zhang, Huifang Li, Huanfeng Shen, and Jie Li. A spatial — spectral adaptive haze removal method for remote sensing images. pages 6134–6137, 2017.

# Appendices

## A. Algorithm implementation

---

### Algorithm 1 Steps of fast image dehazing algorithm

---

**Step 1:** Input an original haze image  $I(x)$  and compute its dark channel image as

$$I^{\text{dark}}(\mathbf{x}) = \min_{\mathbf{y} \in \Omega(\mathbf{x})} \left( \min_{c \in \{r,g,b\}} I^c(\mathbf{y}) \right),$$

where  $I^c(\mathbf{x})$  represents a color channel of the input image,  $\Omega(\mathbf{x})$  is a local patch centered in pixel  $\mathbf{x}$  and the patch size in our paper is  $4 \times 4$ . **Step 2:** Estimate the global atmospheric light

$$\mathbf{A} = \mathbf{I}(\mathbf{x}_k),$$

where

$$\mathbf{x}_k = \arg_{\mathbf{x}} \max(I^{\text{dark}}(\mathbf{x})).$$

**Step 3:** Normalize the haze imaging model by  $A^c$  in each color channel

$$\frac{I^c(\mathbf{x})}{A^c} = \frac{J^c(\mathbf{x})}{A^c} t(\mathbf{x}) + V(\mathbf{x}).$$

Then restrict the normalized image  $\frac{I^c(\mathbf{x})}{A^c}$  into  $[0, 1]$  with linear stretch method. **Step 4:** Estimate the atmospheric veil roughly as

$$\tilde{V}(\mathbf{x}) = \min_{c \in \{r,g,b\}} \frac{I^c(\mathbf{x})}{A^c}.$$

**Step 5:** Refine the coarse atmospheric veil using a low-pass Gaussian filter

$$V(\mathbf{x}) = \frac{1}{W^g} \sum_{\mathbf{y} \in S} G_\sigma(\|\mathbf{x} - \mathbf{y}\|) \tilde{V}(\mathbf{y}),$$

where  $W^g$  is the sum weight of the local patch centered at pixel  $\mathbf{x}$

$$W^g = \sum_{\mathbf{y} \in S} G_\sigma(\|\mathbf{x} - \mathbf{y}\|).$$

Then the transmission is

$$t(\mathbf{x}) = 1 - V(\mathbf{x}).$$

**Step 6:** Restore the scene radiance

$$\mathbf{J}(\mathbf{x}) = \mathbf{A} \times \frac{\mathbf{I}(\mathbf{x}) / \mathbf{A} - kV(\mathbf{x})}{\max(t(\mathbf{x}), t_0)}.$$


---